

# 2+1 Flavor Polyakov–Nambu–Jona-Lasinio Model at Finite Temperature and Nonzero Chemical Potential

Wei-jie Fu<sup>1</sup>, Zhao Zhang<sup>1,2</sup>, and Yu-xin Liu<sup>1,2,3\*</sup>

<sup>1</sup> Department of Physics and the State Key Laboratory of Nuclear Physics and Nuclear Technology, Peking University, Beijing 100871, China

<sup>2</sup> CCAST (World Laboratory), P.O. Box 8730, Beijing 100080, China

<sup>3</sup> Center of Theoretical Nuclear Physics, National Laboratory of Heavy Ion Accelerator, Lanzhou 730000, China

September 3, 2018

## Abstract

We extend the Polyakov-loop improved Nambu–Jona-Lasinio (PNJL) model to 2+1 flavor case to study the chiral and deconfinement transitions of strongly interacting matter at finite temperature and nonzero chemical potential. The Polyakov-loop, the chiral susceptibility of light quarks ( $u$  and  $d$ ) and the strange quark number susceptibility as functions of temperature at zero chemical potential are determined and compared with the recent results of Lattice QCD simulations. We find that there is always an inflection point in the curve of strange quark number susceptibility accompanying the appearance of the deconfinement phase, which is consistent with the result of Lattice QCD simulations. Predictions for the case at nonzero chemical potential and finite temperature are made as well. We give the phase diagram in terms of the chemical potential and temperature and find that the critical endpoint (CEP) moves down to low temperature and finally disappears with the decrease of the strength of the 't Hooft flavor-mixing interaction.

**PACS Numbers:** 12.38.Aw, 11.30.Rd, 12.38.Lg

---

\*corresponding author

# 1 Introduction

QCD phase diagram and thermodynamics has been a subject of intense investigation in recent years. Lattice QCD simulation is a principal approach to explore the qualitative features of strongly interacting matter and make quantitative prediction of its properties. Over the years, this formulation has given us a wealth of information about the phase diagram and thermodynamics at finite temperature and limited chemical potential (see for example Refs. [1–16]). In response to the Lattice QCD simulations, many phenomenological approaches in terms of effective degrees of freedom have been developed to give interpretation of the available Lattice data and further to make prediction in the region of phase diagram that can't be reached by the Lattice QCD.

A promising ansatz of this sort approach is the Polyakov-loop improved Nambu–Jona-Lasinio model (PNJL) [17–20], which combines the two principal non-perturbative features of low-energy QCD: confinement and spontaneous chiral symmetry breaking in a simple formalism. The validity of PNJL model has been tested in a series works by confronting the PNJL results with the Lattice QCD data [20–24]. It has been reported that the 2 flavor ( $u$  and  $d$  quarks) PNJL model can reproduce the result that the crossovers for deconfinement phase transition and the chiral phase transition almost coincide [19, 20]. For finite chemical potential, further investigations suggest that the thermodynamics and susceptibilities obtained in PNJL model are perfectly in agreement with the corresponding Lattice QCD data [20–22]. Recently, the impact of Polyakov-loop dynamics on the color superconductivity phase transition and on the pion superfluidity phase transition within PNJL have been explored in Refs. [23] and [24], respectively.

Although the entanglement of the chiral and the Polyakov-loop dynamics turns out to be indispensable to understand the nature of QCD phase transitions and thermodynamical behavior, the investigations based on this idea up to now are all performed for the two flavor case with small current quark mass so far. Whether the synthesis of Polyakov-loop dynamics with the NJL model when including strange quark works well is still unknown. Nevertheless, the study of the critical temperature of the 2+1 flavor QCD phase transition by the Lattice QCD simulations with physical masses in the continuum limit have recently been reported [15, 25]. Therefore it is interesting to extend the 2 flavor PNJL model to the 2+1 flavor (i.e., including not only  $u$ ,  $d$  quarks, but also  $s$  quark) case to compare with the recent results of the Lattice simulations. In addition, it is worth investigating the 2+1 flavor QCD

phase diagram at finite baryon chemical potential in the NJL model with Polyakov-loop.

One should note that, in the absence of dynamical quarks, the Polyakov-loop expectation value can be taken as an order parameter to identify the color confinement and deconfinement in pure gauge theories (see for example Refs. [17–20]). With the introduction of dynamical quarks with physical masses, the exact  $Z(N_c)$  center symmetry for the gauge fields is lost and the Polyakov-loop is no longer an exact order parameter for the transition from the low temperature, confined phase, to the high temperature, deconfined phase. However, with the distribution function of the quark states, the Polyakov-loop expectation value can still describe the evolution from color-singlet tri-quark state to color-triplet single quark state. Moreover, the results of Lattice QCD [15] show that the Polyakov-loop is also an useful quantity to locate the crossover for deconfinement. Then, the terminology “confinement” we take here is the statistical suppression of the color-triplet quark propagation, but not the dynamical quark confinement. Similarly, the chiral symmetry is explicitly broken by the nonvanishing current masses of quarks. However the chiral condensate is also useful to indicate the chiral crossover.

The purpose of this paper is to extend the 2 flavor PNJL model to 2+1 flavor case to explore the QCD thermodynamics and phase diagram at finite temperature and nonzero chemical potential. The focuses are concentrated on the validity of 2+1 flavor PNJL at finite temperature in comparison with Lattice QCD data and its predictions for the case at nonzero chemical potential and finite temperature. The paper is organized as follows. In Section 2, we extend the PNJL model to the case of 2+1 flavors. In Section 3, we discuss the phase transition of strongly interacting matter at finite temperature and zero chemical potential by analyzing the Polyakov-loop, the chiral susceptibility of light quarks, the strange quark number susceptibility and other related quantities as functions of temperature at zero chemical potential and comparing the results with those of Lattice QCD simulations. In Section 4, we make predictions for the phase transitions in the case at nonzero chemical potential and finite temperature and give a phase diagram of the strongly interacting matter in terms of the temperature and chemical potential. Finally, in Section 5, we give a summary and conclusion.

## 2 The 2+1 Flavor PNJL Model

Following Ref. [20], we extend the 2 flavor Polyakov-loop improved NJL model to include the strange quark and the 2+1 flavor NJL model [26] with a Polyakov-loop can then be given as

$$\begin{aligned} \mathcal{L}_{PNJL} = & \bar{\psi} (i\gamma_\mu D^\mu + \gamma_0 \hat{\mu} - \hat{m}_0) \psi + G \sum_{a=0}^8 \left[ (\bar{\psi} \tau_a \psi)^2 + (\bar{\psi} i\gamma_5 \tau_a \psi)^2 \right] \\ & - K \left[ \det_f (\bar{\psi} (1 + \gamma_5) \psi) + \det_f (\bar{\psi} (1 - \gamma_5) \psi) \right] - \mathcal{U}(\Phi, \Phi^*, T), \end{aligned} \quad (1)$$

where  $\psi = (\psi_u, \psi_d, \psi_s)^T$  is the three-flavor quark field,

$$D^\mu = \partial^\mu - iA^\mu \quad \text{with} \quad A^\mu = \delta_0^\mu A^0 \quad , \quad A^0 = g\mathcal{A}_a^0 \frac{\lambda_a}{2} = -iA_4. \quad (2)$$

$\lambda_a$  are the Gell-Mann matrices in color space.  $\hat{m}_0 = \text{diag}(m_u, m_d, m_s)$  is the three-flavor current quark mass matrix. Throughout this work, we take  $m_u = m_d \equiv m_l$ , assuming the isospin symmetry is reserved on the Lagrangian level, whereas  $m_s$  is usually different from  $m_l$ , thus the  $SU(3)_f$  symmetry is explicitly broken. The quark chemical potential matrix  $\hat{\mu}$  is chosen to be proportional to the unit matrix in our work for simplicity, namely, these three flavor quarks have identical chemical potential  $\mu$ . In the above PNJL Lagrangian, the four-point interaction term with an effective coupling strength  $G$  is  $U(3)_L \otimes U(3)_R$  symmetric, where  $\tau_0 = \sqrt{\frac{2}{3}}1_f$  and  $\tau_a, a = 1, \dots, 8$  are the eight Gell-Mann matrices in flavor space. The flavor-mixing term with coupling strength  $K$  is a determinant in flavor space, which corresponds to the 't Hooft interaction. It breaks the  $U_A(1)$  symmetry and leaves  $SU(3)_L \otimes SU(3)_R$  unbroken.  $\mathcal{U}(\Phi, \Phi^*, T)$  is the Polyakov-loop effective potential.

The above description shows apparently that the degrees of freedom for temporal gauge field expressed in a spatially homogeneous background field is explicitly included in the PNJL model, compared with the conventional NJL model. The Polyakov-loop dynamics represented by this background field is controlled by the Polyakov-loop effective potential  $\mathcal{U}(\Phi, \Phi^*, T)$  and the quarks which couple to the Polyakov-loop. This effective potential can be expressed in terms of the Polyakov-loop expectation value (or, in other words, the traced Polyakov-loop)  $\Phi = (\text{Tr}_c L)/N_c$  and its conjugate  $\Phi^* = (\text{Tr}_c L^\dagger)/N_c$  with the Polyakov-loop  $L$  being a matrix in color space given explicitly by [20]

$$L(\vec{x}) = \mathcal{P} \exp \left[ i \int_0^\beta d\tau A_4(\vec{x}, \tau) \right] = \exp [i\beta A_4], \quad (3)$$

with  $\beta = 1/T$  being the inverse of temperature and  $A_4 = iA^0$ . In the so-called Polyakov gauge, the Polyakov-loop matrix can be given as a diagonal representation [19]. The coupling between Polyakov-loop and quarks is uniquely determined by the covariant derivative  $D_\mu$  in the PNJL Lagrangian in Eq. (1). The trace of the Polyakov-loop,  $\Phi$  and its conjugate,  $\Phi^*$ , can be handled with classical field variables in the PNJL.

Temperature dependent effective potential  $\mathcal{U}(\Phi, \Phi^*, T)$  is taken to reproduce the thermodynamical behavior of the Polyakov-loop for the pure gauge case in accordance with Lattice QCD predictions, and it has the  $Z(3)$  center symmetry like the pure gauge QCD Lagrangian. This  $Z(3)$  center symmetry is spontaneously broken when temperature is above some critical point ( $T_0 \simeq 270$  MeV in pure gauge QCD [20]) and the traced Polyakov-loop develops a finite value. In the absence of quarks,  $\Phi = \Phi^*$  and the Polyakov-loop serves as an order parameter for the deconfinement exactly.

In previous works, two possible forms for the Polyakov-loop effective potential have been well developed. One is a polynomial in  $\Phi$  and  $\Phi^*$  [20], which is denoted by  $\mathcal{U}_{pol}(\Phi, \Phi^*, T)$  in this work and another is an improved effective potential in which the higher order polynomial terms in  $\Phi$  and  $\Phi^*$  are replaced by a logarithm [22, 23]. We denote this improved effective potential by  $\mathcal{U}_{imp}(\Phi, \Phi^*, T)$ . Both effective potentials are taken in the present work to investigate whether our results depend on the details of the Polyakov-loop effective potential. These two effective potentials have the following forms

$$\frac{\mathcal{U}_{pol}(\Phi, \Phi^*, T)}{T^4} = -\frac{b_2(T)}{2}\Phi^*\Phi - \frac{b_3}{6}(\Phi^3 + \Phi^{*3}) + \frac{b_4}{4}(\Phi^*\Phi)^2, \quad (4)$$

with

$$b_2(T) = a_0 + a_1 \left(\frac{T_0}{T}\right) + a_2 \left(\frac{T_0}{T}\right)^2 + a_3 \left(\frac{T_0}{T}\right)^3, \quad (5)$$

and

$$\frac{\mathcal{U}_{imp}(\Phi, \Phi^*, T)}{T^4} = -\frac{1}{2}a(T)\Phi^*\Phi + b(T) \ln [1 - 6\Phi^*\Phi + 4(\Phi^{*3} + \Phi^3) - 3(\Phi^*\Phi)^2], \quad (6)$$

with

$$a(T) = a_0 + a_1 \left(\frac{T_0}{T}\right) + a_2 \left(\frac{T_0}{T}\right)^2, \quad b(T) = b_3 \left(\frac{T_0}{T}\right)^3. \quad (7)$$

A precise fit of the parameter  $a_i$  and  $b_i$  in these two effective potentials has recently been performed to reproduce the Lattice QCD data for pure gauge QCD thermodynamics and the behavior of the Polyakov-loop as a function of temperature in Refs. [20] and [23], respectively. In these two works,  $T_0 = 270$  MeV is chosen to be the critical temperature for the deconfinement to take place in the pure gauge QCD.

After performing the mean field approximation for the Lagrangian of the three-flavor PNJL in Eq. (1), we obtain the thermodynamical potential density as

$$\begin{aligned}
\Omega = & \mathcal{U}(\Phi, \Phi^*, T) + 2G(\phi_u^2 + \phi_d^2 + \phi_s^2) - 4K\phi_u\phi_d\phi_s \\
& - 2 \int \frac{d^3p}{(2\pi)^3} \left\{ 3(E_u + E_d + E_s) \theta(\Lambda^2 - p^2) \right. \\
& + T \ln [1 + 3\Phi e^{-(E_u - \mu)/T} + 3\Phi^* e^{-2(E_u - \mu)/T} + e^{-3(E_u - \mu)/T}] \\
& + T \ln [1 + 3\Phi^* e^{-(E_u + \mu)/T} + 3\Phi e^{-2(E_u + \mu)/T} + e^{-3(E_u + \mu)/T}] \\
& + T \ln [1 + 3\Phi e^{-(E_d - \mu)/T} + 3\Phi^* e^{-2(E_d - \mu)/T} + e^{-3(E_d - \mu)/T}] \\
& + T \ln [1 + 3\Phi^* e^{-(E_d + \mu)/T} + 3\Phi e^{-2(E_d + \mu)/T} + e^{-3(E_d + \mu)/T}] \\
& + T \ln [1 + 3\Phi e^{-(E_s - \mu)/T} + 3\Phi^* e^{-2(E_s - \mu)/T} + e^{-3(E_s - \mu)/T}] \\
& \left. + T \ln [1 + 3\Phi^* e^{-(E_s + \mu)/T} + 3\Phi e^{-2(E_s + \mu)/T} + e^{-3(E_s + \mu)/T}] \right\}, \tag{8}
\end{aligned}$$

where  $\mu$  is the chemical potential,  $T$  is the temperature,  $\phi_i$  is the chiral condensate of quarks with flavor  $i$ , and  $E_i = \sqrt{p^2 + M_i^2}$  is its corresponding quasiparticle energy, with constituent masses for the quark of flavor  $i$

$$M_i = m_i - 4G\phi_i + 2K\phi_j\phi_k. \tag{9}$$

As mentioned above, the breaking of the isospin symmetry is neglected throughout this work. We have thus  $\phi_u = \phi_d \equiv \phi_l$  in the absence of isospin chemical potential.

Minimizing the thermodynamical potential in Eq. (8) with respect to  $\phi_l$ ,  $\phi_s$ ,  $\Phi$ , and  $\Phi^*$ , we obtain a set of equations of motion

$$\frac{\partial \Omega}{\partial \phi_l} = 0, \quad \frac{\partial \Omega}{\partial \phi_s} = 0, \quad \frac{\partial \Omega}{\partial \Phi} = 0, \quad \frac{\partial \Omega}{\partial \Phi^*} = 0. \tag{10}$$

This set of equations can be solved for the fields as functions of temperature  $T$  and chemical potential  $\mu$ . It has been shown in Ref. [20] that, in 2 flavor PNJL model, there is  $\Phi = \Phi^*$  when the quark chemical potential is vanishing ( $\mu = 0$ ). While for  $\mu \neq 0$ ,  $\Phi$  and  $\Phi^*$  have different values.

In the NJL sector of this model, five parameters need to be determined. In our present work we adopt the parameter set in Ref. [27],  $m_l = 5.5$  MeV,  $m_s = 140.7$  MeV,  $G\Lambda^2 = 1.835$ ,  $K\Lambda^5 = 12.36$  and  $\Lambda = 602.3$  MeV, which is fixed by fitting  $m_\pi = 135.0$  MeV,  $m_K = 497.7$  MeV,  $m_{\eta'}$  = 957.8 MeV and  $f_\pi = 92.4$  MeV.

### 3 Phase Transition in the Case of $\mu = 0$ and $T \neq 0$

It has been strongly suggested by current Lattice QCD simulations that the transition from low temperature hadronic phase to high temperature quark-gluon-plasma (QGP) phase at vanishing quark chemical potential is a continuous, non-singular but rapid crossover [16, 28]. It has also been demonstrated that because of the non-singularity of the crossover, different observables lead to various values of transition temperature ( $T_c$ ) in the 2+1 flavor QCD with physical masses both for the light quarks  $m_l$  and for the strange quark  $m_s$  even in the continuum and thermodynamical limit [15]. In order to determine the critical temperature  $T_c$  at vanishing quark chemical potential in the 2 + 1 flavor PNJL model, we consider three quantities, which were used to locate the transition point in the Lattice QCD simulations in Ref. [15], the traced Polyakov-loop (i.e., the Polyakov-loop expectation value. In the following we just denote it as Polyakov-loop for simplicity), the light quark chiral susceptibility and the strange quark number susceptibility.

The chiral susceptibility of the light quark is defined as

$$\chi_l = -\frac{\partial^2 \Omega}{\partial m_l^2}. \quad (11)$$

In order to obtain a dimensionless quantity and renormalize the divergence of the thermodynamical potential  $\Omega$  in Lattice QCD simulations, this quantity was normalized to the following one [15]:

$$\frac{m_l^2 \Delta \chi_l}{T^4} = \frac{m_l^2}{T^4} [\chi_l(T) - \chi_l(0)]. \quad (12)$$

In the PNJL model we have

$$\begin{aligned} \frac{m_l^2 \chi_l}{T^4} = & \frac{6m_l^2}{T^4} \int \frac{d^3 p}{(2\pi)^3} \theta(\Lambda^2 - p^2) \left\{ \frac{p^2}{E_l^3} [1 - 2f(E_l, T, \Phi)] \right. \\ & \left. + \frac{2}{T} \left( \frac{M_l}{E_l} \right)^2 \left[ \frac{\Phi e^{-E_l/T} + 4\Phi e^{-2E_l/T} + 3e^{-3E_l/T}}{A(E_l, T, \Phi)} - 3f^2(E_l, T, \Phi) \right] \right\}, \quad (13) \end{aligned}$$

with  $A(x, T, \Phi)$  and  $f(x, T, \Phi)$  being defined as

$$A(x, T, \Phi) = 1 + 3\Phi e^{-x/T} + 3\Phi e^{-2x/T} + e^{-3x/T}, \quad (14)$$

and

$$f(x, T, \Phi) = \frac{\Phi e^{-x/T} + 2\Phi e^{-2x/T} + e^{-3x/T}}{1 + 3\Phi e^{-x/T} + 3\Phi e^{-2x/T} + e^{-3x/T}}, \quad (15)$$

respectively. Here, we do not distinguish  $\Phi$  and  $\Phi^*$ , because they have the same value at  $\mu = 0$ .

The strange quark number susceptibility is defined as [29]

$$\frac{\chi_s}{T^2} = -\frac{1}{T^2} \left. \frac{\partial^2 \Omega}{\partial \mu_s^2} \right|_{\mu_s=0}, \quad (16)$$

and in the PNJL model given explicitly by

$$\frac{\chi_s}{T^2} = \frac{12}{T^3} \int \frac{d^3 p}{(2\pi)^3} \left[ \frac{\Phi e^{-E_s/T} + 4\Phi e^{-2E_s/T} + 3e^{-3E_s/T}}{A(E_s, T, \Phi)} - 3f^2(E_s, T, \Phi) \right]. \quad (17)$$

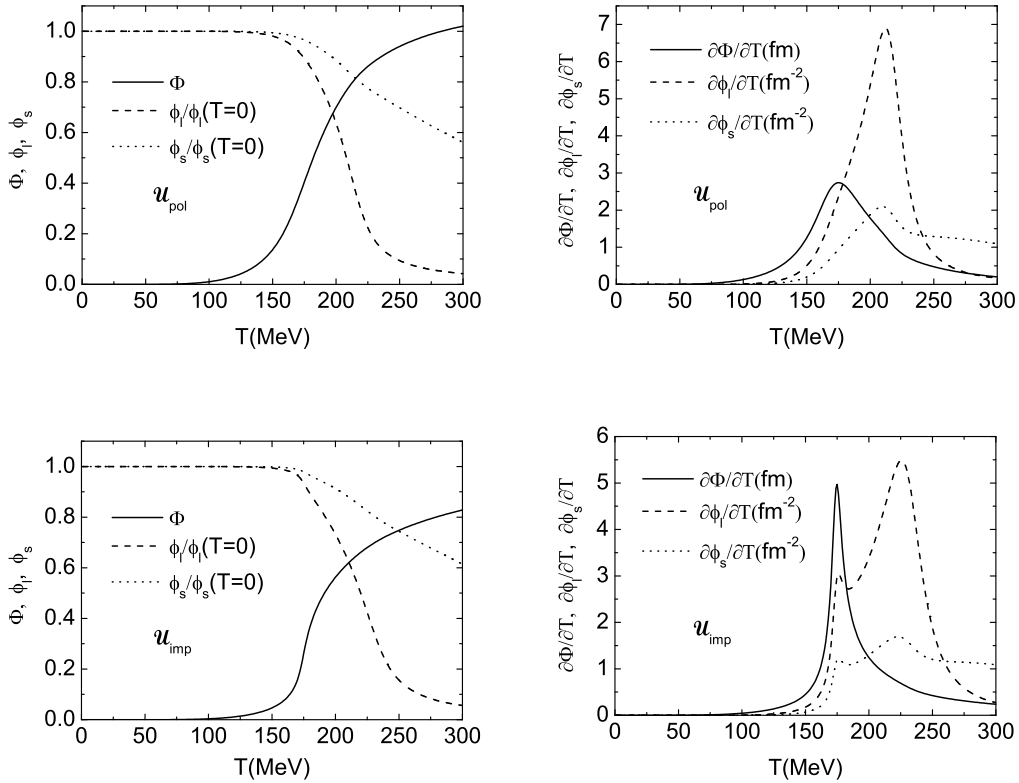


Figure 1: Left panel: calculated Polyakov-loop  $\Phi$ , scaled chiral condensates for light quarks  $\phi_l$  and for strange quarks  $\phi_s$  as functions of temperature at vanishing quark chemical potential in the case of considering the polynomial Polyakov-loop effective potential  $\mathcal{U}_{pol}$ , the improved Polyakov-loop effective potential  $\mathcal{U}_{imp}$ , respectively. Right panel: calculated temperature dependence of the derivatives  $\partial\Phi/\partial T$ ,  $\partial\phi_l/\partial T$  and  $\partial\phi_s/\partial T$  with the two kinds of Polyakov-loop potentials.

The calculated results of the temperature dependence of the Polyakov-loop, the light quark chiral condensate and the strange quark chiral condensate at zero quark chemical



potential with the usual polynomial Polyakov-loop effective potential  $\mathcal{U}_{pol}$  and the improved Polyakov-loop effective potential  $\mathcal{U}_{imp}$  are shown in the left panel of Fig. 1. As we can see, when quarks (including the light and the strange) have physical current masses, the chiral phase evolution is not a true phase transition but a continuous crossover. At the same time, the coupling of the Polyakov-loop to quarks turns the first-order deconfinement transition for the pure-gauge QCD into a crossover as the same as that in the two flavor PNJL case [20]. To determine the pseudo-transition temperature, we have also calculated the derivatives of the Polyakov-loop and the chiral condensates with respect to temperature. The obtained results with the two kinds of Polyakov-loop effective potentials are illustrated in the right panel of Fig. 1. In order to confront our results to those in the Lattice QCD simulations with physical masses for the 2+1 flavor QCD [15], we have rescaled the parameter  $T_0$  in  $\mathcal{U}_{pol}$  from 270 to 200 MeV and in  $\mathcal{U}_{imp}$  from 270 to 215 MeV along the way taken in Ref.[20]. After such a rescaling, we observe that both the Polyakov-loop effective potentials give the same pseudo-deconfinement transition temperature 175 MeV (see right panel of Fig. 1). This value is consistent with the Lattice QCD result  $T_c(P) = 176(3)(4)$  MeV [15], where the numbers in the parenthesis indicate the errors.

After rescaling the  $T_0$  in the effective potential, we can determine the pseudo-critical point  $T_c$  for the chiral phase transition with other quantities. From the appearance of the peaks of  $\partial\phi_l/\partial T$  and  $\partial\phi_s/\partial T$  shown in the right panel of Fig. 1, one can infer that the pseudo-critical temperature of the chiral phase transition for light quarks  $T_c(l)$  are almost the same as that of strange quark  $T_c(s)$ . Such a similarity is quite natural due to the flavor-mixing interaction in the Lagrangian shown in Eq. (1). In more details, the critical temperatures obtained from the polynomial effective potential are  $T_c(l) = 212$  MeV and  $T_c(s) = 210$  MeV, while the corresponding temperatures from the improved effective potential are 226 MeV and 223 MeV. These values are all relatively larger than the recent Lattice QCD results, which are  $T_c(\chi_l) = 192(7)(4)$  MeV in Ref. [25],  $151(3)(3)$  MeV in Ref. [15] and  $169(12)(4)$  MeV in Ref. [29]. This feature is the same as the standard NJL model which also has relatively larger chiral transition temperature [30].

Comparing the upper panel with the lower panel of Fig. 1, one can find that the Polyakov-loop corresponding to the improved effective potential changes more rapidly near the  $T_c(P)$  than that relevant to the polynomial effective potential. The peak of  $\partial\Phi/\partial T$  in the lower-right panel of Fig. 1 is much narrower and higher, which induces two little bumps in the curves of  $\partial\phi_l/\partial T$  and  $\partial\phi_s/\partial T$  at  $T_c(P)$ , while there is no such bump in the curves in the upper-right

panel of Fig. 1 for the polynomial effective potential. These phenomena indicate that, for the improved effective potential, the deconfinement transition has an obvious influence on the chiral condensate.

One may have a question about why the peak of the temperature derivative of the Polyakov-loop  $\Phi$  obtained in the improved effective potential is much narrower than that given by the polynomial effective potential. To explore the underlying physics, we recall that, once the dynamical quarks with physical masses are introduced, the  $Z(3)$  center symmetry is explicitly broken, so that deconfinement phase transition changes from a first order one in pure gauge theories to a crossover. It is then natural that the temperature derivative of the Polyakov-loop smears to a peak with finite height and finite width. The calculated results shown in Fig. 1 manifest that both the polynomial effective potential and the improved effective potential give definitely the temperature derivative of the Polyakov-loop peaks with finite width and finite height. It indicates that both the effective potentials represent the dynamics correctly in some sense. As for that the width given by the improved effective potential is narrower, we should note that recent Lattice QCD results show that the normalized pressure for full QCD with dynamical fermions looks the same as that in the pure gauge theories [28], which indicates that it may be the dynamics of gluons that drives the QCD phase transition, but not that of the fermions [31]. And the crossover of the phase evolution is a quite rapid one [16, 28]. The improved effective potential replaces the higher order terms in  $\Phi$  and  $\Phi^*$  in the polynomial effective potential by the logarithm of the Jacobi determinant which results from integrating out the six non-diagonal Lie algebra directions while keeping the two diagonal ones to represent  $\Phi$  [19, 22, 23]. It means that, the improved effective potential describes the dynamics of the Polyakov-loop (i.e., the gluon dynamics) more appropriately and correlates to the effect of the dynamical quarks more slightly. The narrower width of the deconfinement crossover with the improved effective potential can thus be attributed to that the improved Polyakov-loop effective potential represents better the gluon dynamics.

The calculated results of the temperature dependence of the chiral susceptibility of light quarks are shown in Fig. 2. The pseudo-critical point  $T_c(\chi_l)$  determined from the peak of the chiral susceptibility is 208 MeV for  $\mathcal{U}_{pol}$  and 213 MeV for  $\mathcal{U}_{imp}$ . These values do not exactly coincide with the results of  $T_c(l)$ s shown in Fig. 1, which reflects the nature of the crossover of the phases. However, the discrepancies of the pseudo-critical points from different susceptibilities are within 10 MeV.

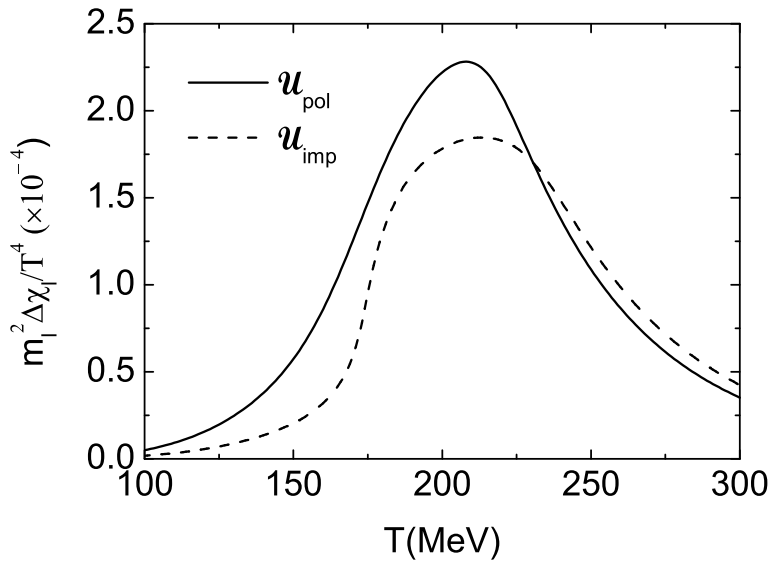


Figure 2: Calculated results of the renormalized chiral susceptibility  $m_l^2 \Delta \chi_l / T^4$  as a function of temperature at zero quark chemical potential for the two Polyakov-loop effective potentials.

Fig. 3 shows the calculated temperature dependence of the strange quark number susceptibility. First of all, we discuss the case including the flavor-mixing effects with  $K\Lambda^5 = 12.36$  in the Lagrangian in Eq. (1). From the calculated results shown as the thinner curves in Fig. 3, one can notice that the  $\chi_s/T^2$  increases monotonically with temperature. Ref. [15] has shown that the pseudo-critical point  $T_c(\chi_s)$  can be defined as the inflection point of a susceptibility curve, viz. the peak of the curve of  $\partial(\chi_s/T^2)/\partial T$ . Our calculated results illustrated in the right panel of Fig. 3 manifest that the location of this pseudo-critical point is affected by both the deconfinement and the chiral crossovers. Because of the common influences by these two crossovers, we find  $T_c(\chi_s) = 203$  MeV for the polynomial potential, which is in the between of the deconfinement pseudo-critical point  $T_c(P) = 175$  MeV and the chiral critical point  $T_c(l) = 212$  MeV,  $T_c(s) = 210$  MeV. This phenomenon is more obvious in the result of the improved effective potential, where a sharp peak appears at the deconfinement transition point  $T_c(P) = 175$  MeV on the curve of  $\partial(\chi_s/T^2)/\partial T$ . It manifests evidently  $T_c(\chi_s) = T_c(P)$ . In addition, the peak is followed by a little platform coming from the contribution of the chiral crossover for light quarks due to the flavor-mixing effects. This phenomenon can be

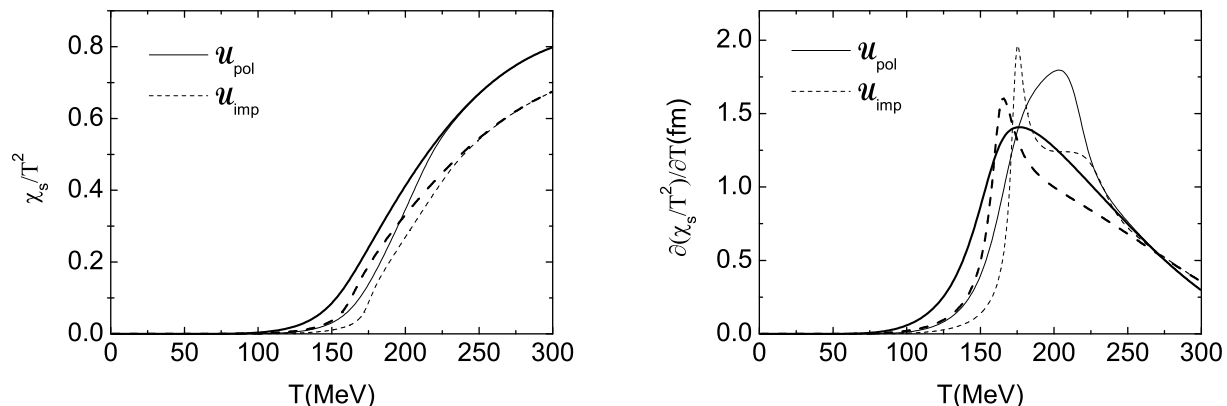


Figure 3: Left panel: calculated results of the scaled strange quark number susceptibility  $\chi_s/T^2$  as a function of temperature (thinner curves are for the case with  $K\Lambda^5 = 12.36$  and thicker ones for  $K\Lambda^5 = 0$ ). Right panel: plots of the calculated  $\partial(\chi_s/T^2)/\partial T$ .

understood as the follows. Being not color-singlets, there are almost no free strange quarks before the deconfinement crossover takes place. As the temperature increases, the crossover for the deconfinement occurs and the strange quark number susceptibility develops to finite values abruptly. In general case, the quasiparticle energy of strange quarks becomes smaller due to the partial reduction of the condensate of strange quarks which is along with the light quarks chiral crossover because of the flavor-mixing interactions. It leads it easier to excite quarks, and in turn to increase the value of the quark number susceptibility. However, since the improved effective potential represents the gluon dynamics better and the deconfinement crossover governed by the gluon dynamics occurs more abruptly as mentioned above, the increasing rate of the strange quark number susceptibility with respect to temperature induced by the deconfinement crossover dominates over that induced by the reduction of the quark condensate at the deconfinement pseudo-critical temperature. As a consequence, the pseudo-critical temperature given by the strange quark number susceptibility coincides with that for the deconfinement crossover. As the temperature increases further, the reduction of the quasiparticle energy of the quark begins to play the role, it generates then a platform in the curves of  $\partial(\chi_s/T^2)/\partial T$ . In order to study the influence of the deconfinement crossover on the  $\chi_s$  further we turn off the flavor-mixing interaction by setting  $K\Lambda^5 = 0$ . The obtained results are illustrated in the thicker curves in Fig. 3. We find again that  $\chi_s/T^2$  gradually develops a finite value with the appearance of the deconfinement phase. Since the  $\chi_s/T^2$  is no longer influenced by the light quark chiral crossover any more, the difference between the

pseudo-critical temperatures given by the two effective potentials is much smaller than that with the flavor-mixing being taken into account. Furthermore, the curve of  $\partial(\chi_s/T^2)/\partial T$  for the polynomial potential moves down to lower temperature obviously and there are not any platforms on the curve of  $\partial(\chi_s/T^2)/\partial T$  for the improved effective potential. Therefore, we could qualitatively understand the results of Lattice QCD simulations in Ref. [15] that the pseudo-critical point determined from the strange quark number susceptibility is quite close to that determined from the Polyakov loop. Nevertheless, it is not obvious that the quark number susceptibility has any relations with the chiral crossover for light quarks, which maybe indicates that the flavor-mixing interactions are relatively weak at high temperature.

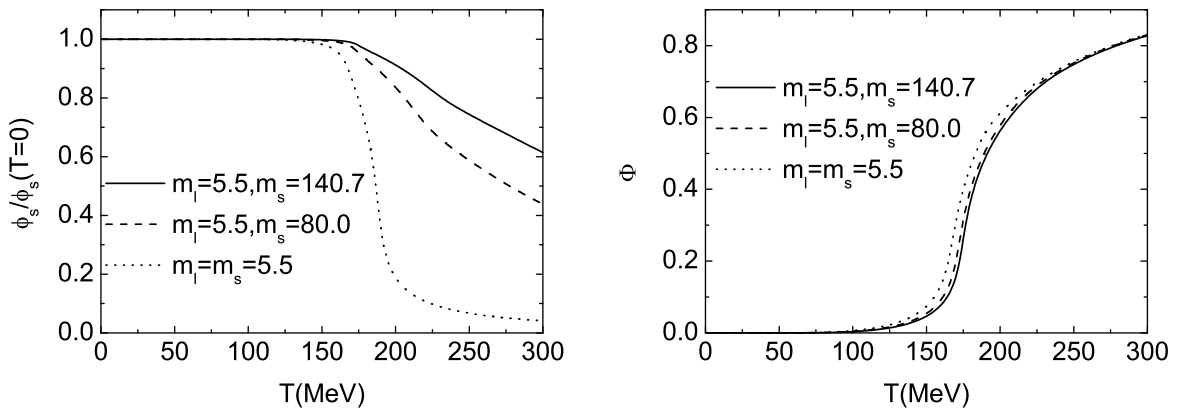


Figure 4: Calculated results of the scaled strange quark chiral condensate as a function of temperature with different values of the current mass of strange quark for the improved effective potential (left panel) and the temperature dependence of the corresponding Polyakov-loop  $\Phi$  at several strange quark masses (right panel).

In order to investigate the influences of the current mass of strange quark on the properties of chiral and deconfinement crossover in the case of including the flavor-mixing effects, we depict the scaled strange quark condensate and the Polyakov-loop as functions of temperature with different values of strange quark current mass in Fig. 4, using the improved effective potential  $\mathcal{U}_{imp}$ . Obviously, one can find from the figure that the chiral crossover is quite sensitive to the variation of the current mass of strange quark. The chiral transition temperature  $T_c(s)$  defined above decreases from about 225 MeV to 188 MeV for the improved effective potential  $\mathcal{U}_{imp}$  when the value of  $m_s$  is reduced from 140.7 MeV to 5.5 MeV. The same thing occurs for the polynomial effective potential  $\mathcal{U}_{pol}$ . Furthermore, the region of crossover for the chiral phase evolution takes place in a more narrow range of temperature.

Nevertheless, as for the deconfinement transition, differences between the physical case with  $m_s = 140.7$  MeV and the hypothetical case with  $m_s = 5.5$  MeV are very small. Consequently, the difference between the chiral pseudo-critical point  $T_c(s)$  and the deconfinement pseudo-critical point  $T_c(P)$  becomes smaller when the current mass of the strange quark decreases.

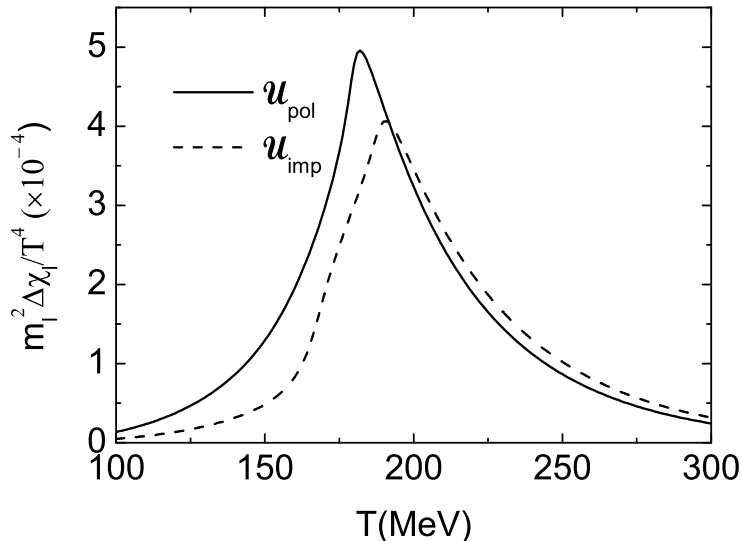


Figure 5: The same as Fig. 2 but with  $m_s = m_l = 5.5$  MeV.

Fig. 5 shows the renormalized chiral susceptibility  $m_l^2 \Delta \chi_l / T^4$  as a function of temperature for the case of  $m_s = m_l = 5.5$  MeV, viz. neglecting the flavor difference. As one expects, the curves in this figure are much narrower and sharper than those in Fig. 2. The chiral pseudo-critical temperature  $T_c(\chi_l)$  is 182 MeV for the  $\mathcal{U}_{pol}$  and 191 MeV for the  $\mathcal{U}_{imp}$ , which are 26 MeV and 22 MeV smaller than their corresponding values for the case with physical strange quark mass, respectively.

We have also calculated the temperature dependence of the strange quark number susceptibility  $\chi_s / T^2$  with  $m_s = m_l = 5.5$  MeV. The obtained results are shown in Fig. 6. From the figure we can recognize not surprisingly,  $T_c(\chi_s) = 179$  MeV for the polynomial effective potential, which is consistent with the chiral pseudo-critical temperature  $T_c(\chi_l) = 182$  MeV and the deconfinement critical temperature  $T_c(P) = 178$  MeV. As for the improved effective potential, there are two peaks located at 169 MeV and 186 MeV in the curve of the temperature

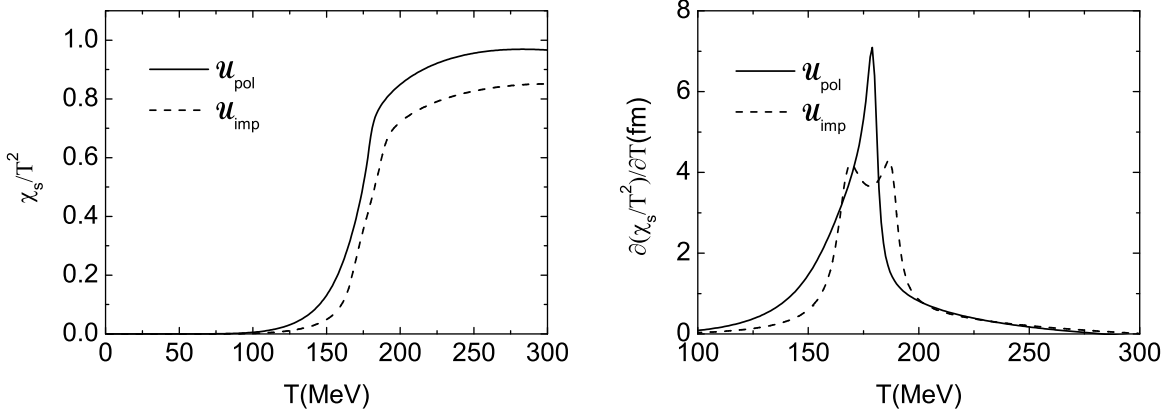


Figure 6: The same as Fig. 3 but with  $m_s = m_l = 5.5$  MeV and  $K\Lambda^5 = 12.36$ .

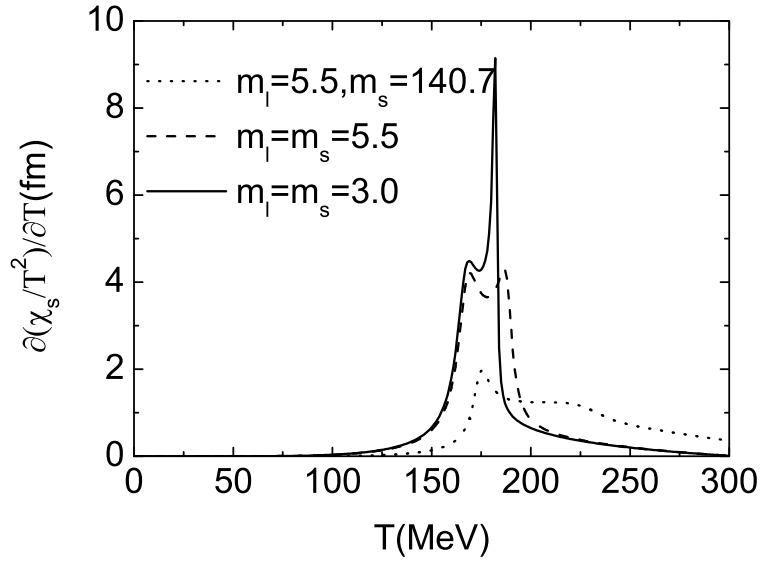


Figure 7: Calculated derivatives of the strange quark number susceptibility versus the temperature in the cases:  $m_l = 5.5$  MeV,  $m_s = 140.7$  MeV;  $m_l = m_s = 5.5$  MeV; and  $m_l = m_s = 3.0$  MeV.

derivative. We have then the pseudo-critical temperature in the case of  $m_s = m_l = 5.5$  MeV,  $T_c(\chi_s) = 169$  MeV, 186 MeV, which correspond to the  $T_c(P) = 168$  MeV,  $T_c(\chi_l) = 188$  MeV, respectively. Fig. 7 shows the temperature derivative of the strange quark number susceptibility for the improved effective potential with several values of current mass of strange

quarks. One can observe from the figure that the peak related to the chiral critical point grows drastically as the current mass of strange quarks decreases from 140.7 MeV to 3.0 MeV.

One should note that in order to confront our results to those in Lattice QCD simulations in [15], we have rescaled the parameter  $T_0$  in  $\mathcal{U}_{pol}$  from 270 to 200 MeV and in  $\mathcal{U}_{imp}$  from 270 to 215 MeV to fix the pseudo-deconfinement transition temperature  $T_c(P) = 175$  MeV. However, recent Lattice QCD simulations [25, 29] show that there are some uncertainties in this pseudo-critical temperature for the 2+1 flavors with physical quark masses, ranging from 150 MeV to 190 MeV. We repeat the calculations above with different values of  $T_0$ , and find that the hierarchy in the pseudo-critical temperatures also exists for the cases with physical masses. For example, if we do not rescale the value of  $T_0$  and keep it being 270 MeV as in the pure gauge field case, we find  $T_c(P) = 212$  MeV and  $T_c(l) = 242$  MeV for the improved effective potential. The difference between these two values are obvious. For the polynomial effective potential this difference becomes smaller but is also obvious with  $T_c(P) = 227$  MeV and  $T_c(l) = 240$  MeV. One interesting thing is that when the value of  $m_s$  is reduced from 140.7 MeV to 5.5 MeV and  $T_0$  is kept at 270 MeV as well, we find that the deconfinement and chiral pseudo-transitions are almost coincident, with  $T_c(P) = 205$  MeV,  $T_c(l) = 211$  MeV for the improved Polyakov-loop effective potential  $\mathcal{U}_{imp}$  and  $T_c(P) = 210$  MeV,  $T_c(l) = 211$  MeV for the polynomial effective potential  $\mathcal{U}_{pol}$ .

## 4 Phase Transition in the Case of $\mu \neq 0$ and $T \neq 0$

In the above sections, we have mentioned that in the presence of quark chemical potential  $\mu$ , the (traced) Polyakov-loop  $\Phi$  and its conjugation  $\Phi^*$  satisfying Eqs. (10) are different from each other. Viz.

$$\Delta\Phi = \frac{\Phi^* - \Phi}{2} \quad (18)$$

develops a finite value. It has also been demonstrated that this difference originates from the sign problem of the fermion determinant at finite density, which is unavoidable not only in Lattice QCD simulations but also in the mean-field approximation [32]. However, it was shown that such a difference between  $\Phi$  and  $\Phi^*$  at finite density may be not of major qualitative importance in determining the phase diagram [20, 33]. Therefore, we use the average value of  $\Phi$  and  $\Phi^*$  to indicate the pseudo-deconfinement phase transition at finite density, viz.

$$\overline{\Phi} = \frac{\Phi^* + \Phi}{2}. \quad (19)$$



Solving the four equations in Eqs. (10), we can obtain  $\Phi$  and  $\Phi^*$  as functions of temperature  $T$  and quark chemical potential  $\mu$ , and in turn the  $\Delta\Phi$  and  $\overline{\Phi}$  defined above. In the following discussions, we are only concerned about quantities  $\Delta\Phi$  and  $\overline{\Phi}$ , therefore,  $\overline{\Phi}$  is just denoted by  $\Phi$  from now on.

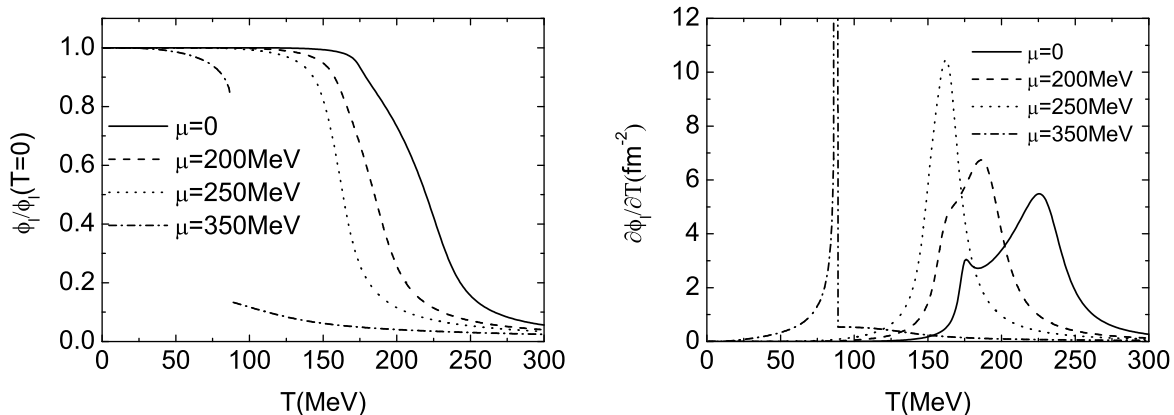


Figure 8: Calculated results of the scaled light quark chiral condensate (left panel) and its derivative with respect to temperature (right panel) as functions of temperature for several values of the quark chemical potential.

In this section only the improved Polyakov-loop effective potential is implemented and  $T_0$  in this potential is also chosen to be 215 MeV. We investigate the cases with physical quark masses ( $m_l = 5.5$  MeV,  $m_s = 140.7$  MeV) and including the flavor-mixing effect ( $K\Lambda^5 = 12.36$ ), and keep other model parameters unchanged (except explicit explanations). Fig. 8 shows the calculated temperature dependence of the light quark condensate and its derivative at several quark chemical potentials. From the figure, one can recognize easily that, with the increase of chemical potential, the pseudo-critical temperature of the chiral transition determined from light quarks decreases and the crossover becomes more and more narrow and abrupt (as shown in the right panel of Fig. 8) and eventually evolves to a first-order transition at the critical endpoint (CEP) ( $T_{CEP} = 128$  MeV,  $\mu_{CEP} = 308$  MeV). From the right panel of Fig. 8, one can also notice that the difference between the chiral pseudo-critical temperature and that for deconfinement becomes small with the increase of  $\mu$ , which means that the chiral phase boundary drops more rapidly than that of the confinement phase does with the increase of chemical potential  $\mu$ . This phenomenon is consistent with the results shown in Figs. 16 and 17 of Ref. [33] for the two-flavor PNJL model.

We have also calculated the temperature and chemical potential dependence of the scaled

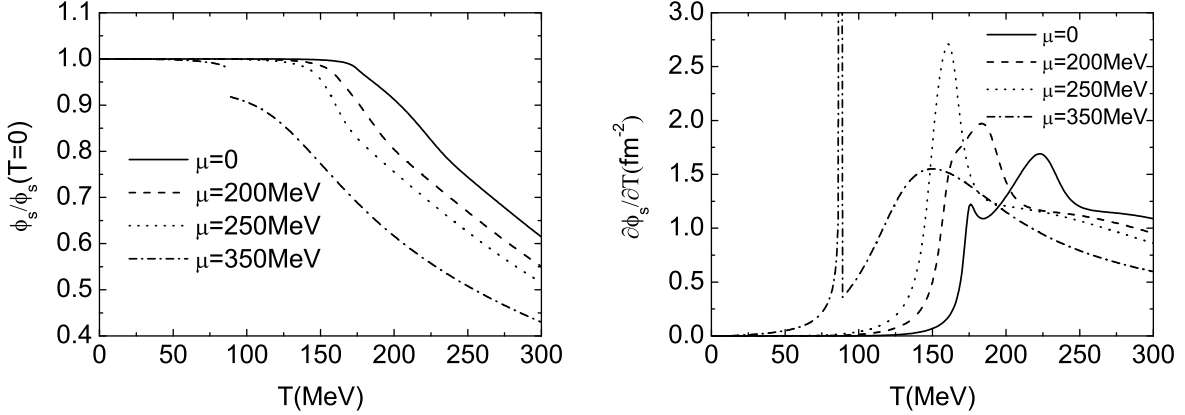


Figure 9: The same as Fig. 8, but for the condensate of strange quarks.

strange quark condensate and its derivative  $\partial\phi_s/\partial T$ . The obtained results in the case of that the chemical potential of strange quarks takes the same values as for the light quark condensate are illustrated in Fig. 9. The figure shows evidently that the curves of  $\partial\phi_s/\partial T$  in the right panel of Fig. 9 have peaks at the same temperature as the curves of  $\partial\phi_l/\partial T$  in the right panel of Fig. 8. This is reasonable because  $\phi_s$  is influenced by  $\phi_l$  through the 't Hooft flavor-mixing interactions. However, higher temperature is needed to reduce the value of  $\phi_s$  to approach zero since the strange quark has much larger current mass. Therefore, we see that there is a broad peak after the restoration of the chiral symmetry for light quarks on the curve of  $\partial\phi_s/\partial T$  with  $\mu = 350$  MeV in the right panel of Fig. 9, which corresponds to the further reduction of the condensate for strange quarks. It should be noticed that there are some uncertainties in the location of the broad peak corresponding to  $\mu = 350$  MeV because of the high chemical potential and temperature, since in these regions, the fermionic distribution function is nonvanishing at momentum beyond the cutoff of the model, which indicates that those regions are out of the scope of NJL-like models.

Fig. 10 represents the calculated Polyakov-loop as a function of temperature at finite quark chemical potential. The figure manifests evidently that the rapid crossover for the deconfinement transition at  $\mu = 0$  is smeared by nonzero  $\mu$  and the crossover gets much flatter and milder. This result is qualitatively consistent with the mean-field result shown in Fig. 10 of Ref. [32]. Fig. 11 shows the  $\Delta\Phi$  at finite quark chemical potential. We have magnified the value of  $\Delta\Phi$  by ten times in order to compare it to the  $\Phi$  conveniently. As one observes that the value of  $\Delta\Phi$  increases with the temperature below the deconfinement pseudo-critical temperature  $T_c(P)$ , while above  $T_c(P)$ , it decreases and approaches to zero.

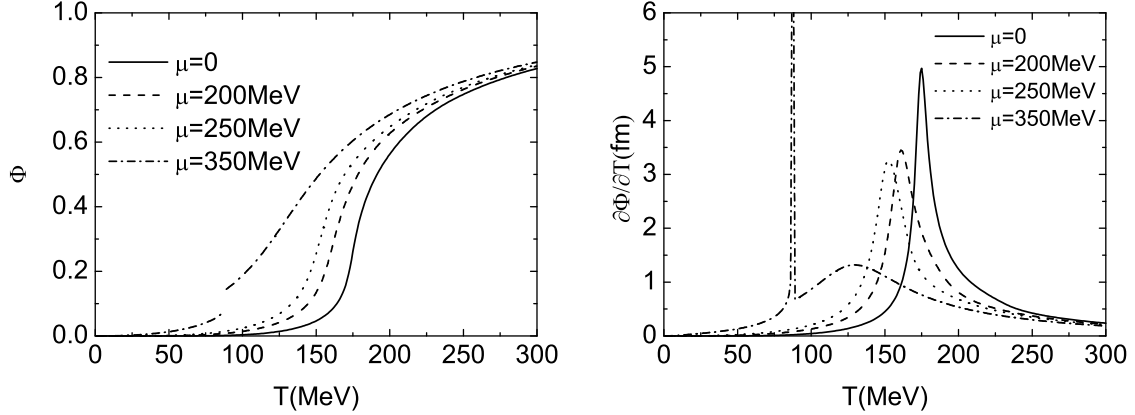


Figure 10: Calculated results of the Polyakov-loop  $\Phi$  (left panel) and  $\partial\Phi/\partial T$  (right panel) as functions of temperature at several values of quark chemical potentials.

To discuss the chemical potential dependence of the phase evolution in detail, we show the calculated quark chemical potential dependence of chiral condensates  $\phi_l$  and  $\phi_s$  at  $T = 100$  MeV in Fig. 12. Since the temperature  $T = 100$  MeV is below the temperature of CEP (128 MeV), the chiral phase transition for light quarks is in first-order, which corresponds to the divergence of the curve of  $\partial\phi_l/\partial\mu$  in the right panel of Fig. 12. Furthermore, besides the influence of the chiral restoration for light quarks due to the flavor-mixing, exhibiting a discontinuity in the curves of  $\phi_l$  and  $\phi_s$ , there is a smooth crossover for further reduction of the strange quark condensate at higher values of the quark chemical potential (the second peak in the curve of  $\partial\phi_s/\partial\mu$  is located at about 450 MeV). We also study the influences of the 't Hooft flavor-mixing strength  $K$  on the strange quark chiral transition with finite quark chemical potential and finite temperature. The calculated results at temperature  $T = 100$  MeV are illustrated in Fig. 13. The figure shows evidently that, as the flavor-mixing strength becomes weaker, the temperature of CEP becomes lower. Consequently, the first-order chiral phase transition of light quarks displaying a discontinuity in the curve of  $\phi_s/\phi_s(T=0)$  in Fig. 13 evolves to a continuous crossover. While at higher chemical potential for further reduction of the strange quark chiral condensate, since the chiral symmetry for light quarks has been restored, the flavor-mixing interactions that couple different flavors of condensates can be neglected. Therefore, these three curves in Fig. 13 coincide with each other at large values of the chemical potential.

We also investigate the quark chemical potential dependence of the Polyakov-loop  $\Phi$  and  $\Delta\Phi$ . The calculated results at several temperatures are illustrated in Fig. 14. Such an

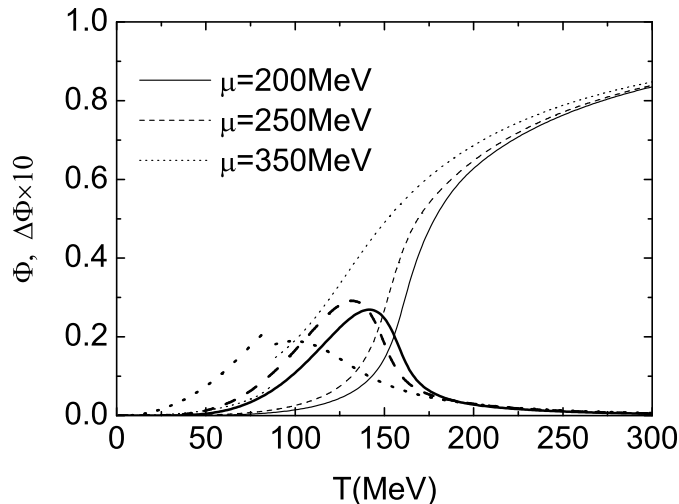


Figure 11: Calculated results of the Polyakov-loop  $\Phi$  (thin curves) and scaled  $\Delta\Phi$  (thick curves) as functions of temperature at several values of the chemical potential.

investigation is extremely interesting if the chemical potential is beyond the scope of the current Lattice QCD simulations. It is easy to infer from the figure that the Polyakov-loop is obviously suppressed at small  $T$  and  $\mu$ . It indicates a tendency of confinement. This tendency is reversed with the increase of  $T$  or  $\mu$ . For example, the value of  $\Phi$  corresponding to  $T = 180$  MeV (the thin dotted curve) is much larger than those corresponding to other two values of the temperature at low  $\mu$ , since  $T = 180$  MeV is higher than the deconfinement pseudo-critical temperature at zero chemical potential ( $T_c(P) = 175$  MeV). The amplified  $\Delta\Phi$  is also shown in Fig. 14, which is much smaller compared with  $\Phi$  in the deconfinement phase.

As a finality, we present the phase diagrams of the 2+1 flavor PNJL in Fig. 15 and discuss their dependence on the flavor-mixing interaction strengths (left panel) and the current masses of quarks (right panel) for the improved Polyakov-loop effective potential. The curves for crossover are determined by the location of the peaks of the derivative of “quasi” order parameters with respect to  $T$  or  $\mu$ . As for the left panel of Fig. 15, the solid, dotted curves indicate the crossover, the first-order chiral transition for light quarks, respectively, separated by the critical endpoint (CEP). The dashed curves correspond to the crossover for the deconfinement and we only depict them in the range of  $\mu = 0 \sim 350$  MeV.

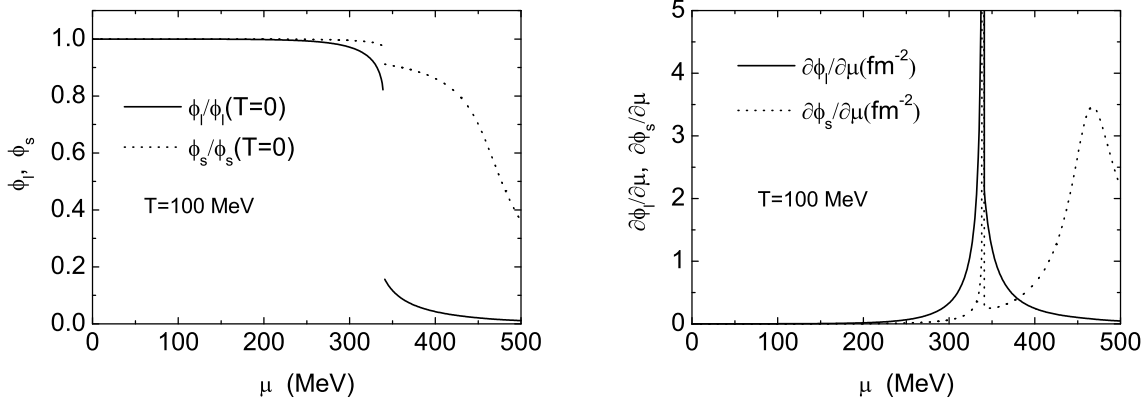


Figure 12: Left panel: calculated quark chemical potential dependence of the scaled chiral condensates  $\phi_l$  and  $\phi_s$  at temperature  $T = 100$  MeV. Right panel: plots of  $\partial\phi_l/\partial\mu$  and  $\partial\phi_s/\partial\mu$  with respect to the chemical potential.

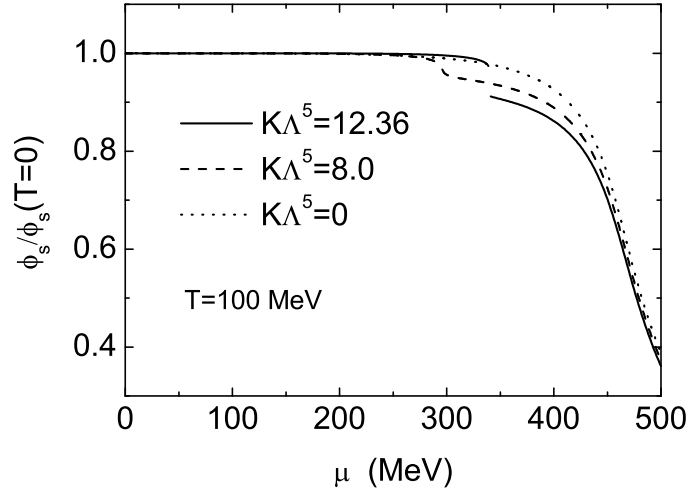


Figure 13: Calculated strange quark condensate as a function of chemical potential with different values of  $K\Lambda^5$  at  $T = 100$  MeV.

The dash-dotted curves indicate the “further chiral crossover” for strange quarks and we only depict them in the temperature range  $T \in [0, 120]$  MeV, because NJL-type models are problematic in the range of large  $\mu$  and high  $T$  as discussed above. One can observe from the figure that, as the strength of flavor-mixing interactions becomes weaker, the CEP moves down to lower temperature. We also find that, when the flavor-mixing interaction strength  $K$

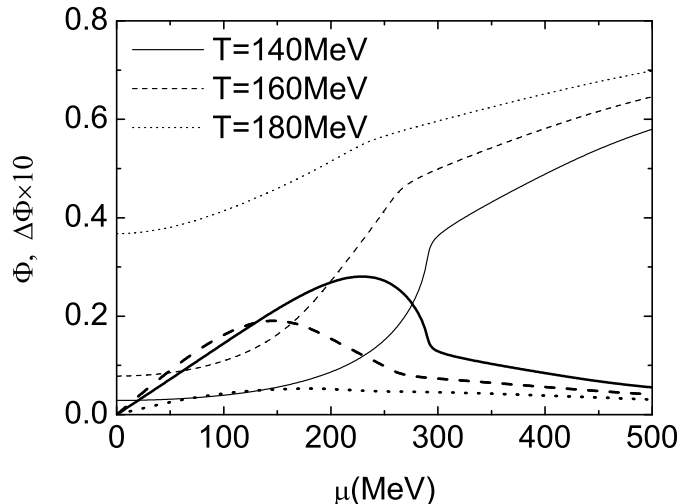


Figure 14: Calculated Polyakov-loop  $\Phi$  (thin curves) and the scaled  $\Delta\Phi$  (thick curves) as functions of quark chemical potential at several values of temperature.

approaches to zero, the CEP moves toward  $\mu$ -axis gradually and finally disappears from the phase diagram. It should be noted that two dash-dotted curves corresponding to two values of  $K\Lambda^5$  coincides with each other because of the reason mentioned above. The same thing occurs for the deconfinement crossover outside the chiral phase boundary of light quarks.

Furthermore, the dependence of the phase diagram on the current mass of quarks has been investigated as well. We neglect differences between the light quarks and the strange quark, and study two cases with  $m_l = m_s = 5.5$  MeV,  $m_l = m_s = 0$ , respectively. Their corresponding phase diagrams are depicted in the right panel of Fig. 15. Here,  $K\Lambda^5 = 12.36$  is chosen. Since the current mass of strange quark is the same as those of light quarks, the strange quark chiral transition coincides with those of light quarks and there is no dash-dotted line in the phase diagram. when the current mass of strange quark is reduced from 140.7 MeV to 5.5 MeV, both the critical value of  $\mu$  at  $T = 0$  and that of  $T$  at  $\mu = 0$  decrease, and the CEP moves toward to the  $T$ -axis. If the values of both  $m_l$  and  $m_s$  are further reduced, for example in the chiral limit, we find that the CEP disappears from the phase diagram and there is only first order chiral transition in the whole range of chemical potential and temperature, which is illustrated by the thinner dotted line in the right panel of Fig. 15. This result is quite consistent with the Pisarski-Wilczek argument [34] that the order of the

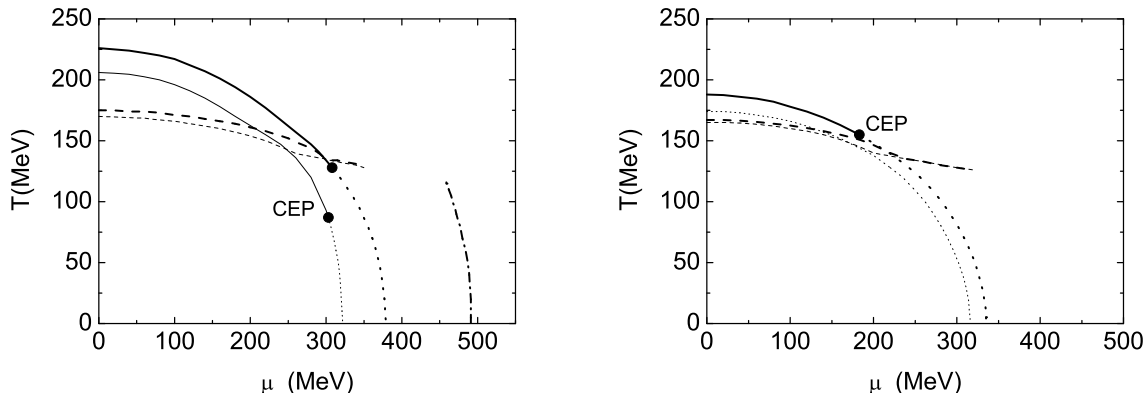


Figure 15: Left panel: calculated phase diagram in terms of temperature and quark chemical potential of the 2+1 flavor PNJL with physical masses, viz.  $m_l = 5.5$  MeV,  $m_s = 140.7$  MeV, and with different flavor-mixing interaction strengths:  $K\Lambda^5 = 12.36$  (thicker curves) and  $K\Lambda^5 = 8.0$  (thinner curves). Right panel: phase diagrams for  $m_l = m_s = 5.5$  MeV (thicker curves) and in the chiral limit  $m_l = m_s = 0$  (thinner curves), respectively, with  $K\Lambda^5$  fixed at 12.36.

temperature driven chiral symmetry restoration transition is first order for three massless quarks. In the framework of the PNJL model, this could be understood as a result of that the thermodynamical potential involves a term cubic in the chiral condensate, because of the 't Hooft interaction. To study the dependence of the phase evolution on the flavor-mixing interaction more thoroughly, we perform a series calculations by reducing the strength of the flavor-mixing interactions gradually and find that when the flavor-mixing interaction strength  $K\Lambda^5$  decreases to a value of about 5, the order of the temperature driven chiral transition is changed from first to second.

## 5 Summary and Conclusions

In summary, we have extended the Polyakov-loop improved NJL model to the 2+1 flavor case with inclusion of strange quark. This 2+1 flavor PNJL is a synthesis of the conventional 2+1 flavor NJL model, which includes the flavor-mixing 't Hooft interaction, and the Polyakov-loop dynamics governed by a Polyakov-loop effective potential. Within the framework of such a model, we have studied the chiral and Polyakov-loop dynamics and their mutual influences to understand the nature of the QCD phase transitions in the three-flavor system.

More concretely, we investigate the chiral and deconfinement crossovers with finite tem-

perature at zero quark chemical potential with physical current mass of strange quark. Three kinds of pseudo-critical temperature corresponding to three different quantities: Polyakov-loop, chiral susceptibility of light quarks and strange quark number susceptibility, are determined in the PNJL model. By employing two Polyakov-loop effective potentials existing in literatures, viz. the polynomial effective potential and the improved one, we all find that different observables lead to different values of transition temperature due to the non-singularity of the crossover, which probably indicate that this phenomenon is independent of the choice of the Polyakov-loop effective potential in the PNJL model. However, other effective potentials need to be developed to verify this result. The hierarchy in the pseudo-critical temperatures found in our model is consistent with the recent Lattice QCD results in Ref. [15]. However,  $T_c(\chi_l)$ ,  $T_c(\chi_s)$  and  $T_c(P)$  found in another Lattice simulation [25] almost coincide and there is not the hierarchy. But we should be careful to use the results in Ref. [25], because the lattice spacings used in Ref. [25] are not in the scaling regime and the results obtained with their lattice spacings can not give a consistent continuum limit for  $T_c$  [15]. Making use of the two different Polyakov-loop effective potentials, we find that there is always an inflection point in the curve of strange quark number susceptibility vs temperature, accompanying the appearance of the deconfinement phase, independent of the strength of flavor-mixing interaction, which is also consistent with the results of Lattice QCD simulations [15]. Effects of the current mass of strange quark ( $m_s$ ) are studied, too. We find that the chiral crossover for light quarks moves down to lower temperature and become more abruptly with the decrease of  $m_s$ , while the deconfinement crossover is almost not influenced by the variation of  $m_s$ .

Furthermore, predictions for nonzero quark (baryon) chemical potential and finite temperature are made in this work. We investigate the temperature and chemical potential dependence of the Polyakov-loop  $\Phi$ ,  $\Delta\Phi$  and the condensates for light quarks and strange quarks as well as their mutual interactions. We find that in the deconfinement phase the value of  $\Phi$  approaches to one and  $\Delta\Phi$  is much smaller than that of  $\Phi$ . We also give the phase diagram of the strongly interacting matter in terms of the chemical potential  $\mu$  and temperature  $T$ . It shows that the critical endpoint (CEP) moves down to the  $\mu$ -axis and finally disappears with the decrease of the strength of the 't Hooft flavor-mixing interaction. On the contrary, the CEP moves toward to the  $T$ -axis as the current mass of strange quarks is reduced and disappears when the chiral limit is approached.

It is well known that the  $U_A(1)$  symmetry of QCD is explicitly broken by the axial



anomaly coming from the gluon dynamics at quantum level. It is very interesting to investigate the effects of the interplay among the  $U_A(1)$  anomaly, the Polyakov-loop dynamics and the chiral symmetry breaking at finite temperature and nonzero chemical potential in the PNJL model. Following Ref. [35] which studies the properties of pion and sigma mesons in the two flavor PNJL model, we can analyze the pseudoscalar mesons and their chiral partners in three flavor case and their convergence could indicate the restoration of the  $U_A(1)$  symmetry with the increase of temperature or chemical potential. These studies are under progress and we will report it elsewhere.

## Acknowledgements

This work was supported by the National Natural Science Foundation of China under contract Nos. 10425521, 10575004 and 10675007, the Major State Basic Research Development Program under contract No. G2007CB815000, the Key Grant Project of Chinese Ministry of Education (CMOE) under contact No. 305001, and the Research Fund for the Doctoral Program of Higher Education of China under grant No 20040001010. One of the authors (Y.X. Liu) would also acknowledge the support of the Foundation for University Key Teacher by the CMOE. Besides, all the authors acknowledge gratefully the stimulating discussions with Dr. Lei Chang and Mr. Guo-yun Shao.

## References

- [1] G. Boyd, J. Engels, F. Karsch, E. Laermann, C. Legeland, M. Lügemeier, and B. Petersson, Nucl. Phys. **B 469**, 419 (1996).
- [2] J. Engels, O. Kaczmarek, F. Karsch, and E. Laermann, Nucl. Phys. **B 558**, 307 (1999).
- [3] Z. Fodor, and S. D. Katz, Phys. Lett. **B 534**, 87 (2002); *ibid*, J. High Energy Phys. **0203**, 014 (2002).
- [4] Z. Fodor, S. D. Katz, and K. K. Szabo, Phys. Lett. **B 568**, 73 (2003).
- [5] C. R. Allton, S. Ejiri, S. J. Hands, O. Kaczmarek, F. Karsch, E. Laermann, Ch. Schmidt, and L. Scorzato, Phys. Rev. **D 66**, 074507 (2002).

- [6] C. R. Allton, S. Ejiri, S. J. Hands, O. Kaczmarek, F. Karsch, E. Laermann, and Ch. Schmidt, Phys. Rev. **D 68**, 014507 (2003).
- [7] C. R. Allton, M. Döring, S. Ejiri, S. J. Hands, O. Kaczmarek, F. Karsch, E. Laermann, and K. Redlich, Phys. Rev. **D 71**, 054508 (2005).
- [8] E. Laermann, and O. Philipsen, Ann. Rev. Nucl. Part. Sci. **53**, 163 (2003).
- [9] P. de Forcrand, and O. Philipsen, Nucl. Phys. **B 642**, 290 (2002); Nucl. Phys. **B 673**, 170 (2003); O. Philipsen, arXiv: hep-lat/0510077; P. de Forcrand, and S. Kratochvila, Nucl. Phys. **B (Proc. Suppl.) 153**, 62 (2006).
- [10] S. Kratochvila, and P. de Forcrand, Nucl. Phys. **B (Proc. Suppl.) 129**, 533 (2004); *ibid*, Nucl. Phys. **B (Proc. Suppl.) 140**, 514 (2005); *ibid*, Phys. Rev. **D 73**, 114512 (2006).
- [11] M. D’Elia, and M. P. Lombardo, Phys. Rev. **D 67**, 014505 (2003).
- [12] M. D’Elia, and M. P. Lombardo, Phys. Rev. **D 70**, 074509 (2004).
- [13] V. Azcoiti, G. Di Carlo, A. Galante, V. Laliena, Nucl. Phys. **B 723** (2005), 77.
- [14] A. Alexandru, M. Faber, I. Hovath, and K.F. Liu, Phys. Rev. **D 72** (2005), 114513.
- [15] Y. Aoki, Z. Fodor, S. D. Katz, and K. K. Szabó, Phys. Lett. **B 643**, 46 (2006).
- [16] Y. Aoki, G. Endrodi, Z. Fodor, S. D. Katz, and K. K. Szabó, Nature **443**, 675 (2006).
- [17] P. N. Meisinger, and M. C. Ogilvie, Phys. Lett. **B 379**, 163 (1996); P. N. Meisinger, T. R. Miller, and M. C. Ogilvie, Phys. Rev. **D 65**, 034009 (2002).
- [18] R. D. Pisarski, Phys. Rev. **D 62**, 111501 (2000); A. Dumitru and R. D. Pisarski, Phys. Lett. **B 504**, 282 (2001), Phys. Lett. **B 525**, 95 (2002), Phys. Rev. **D 66**, 096003 (2002).
- [19] K. Fukushima, Phys. Lett. **B 591**, 277 (2004).
- [20] C. Ratti, M. A. Thaler, and W. Weise, Phys. Rev. **D 73**, 014019 (2006); C. Ratti, M. A. Thaler, and W. Weise, nucl-th/0604025.
- [21] S. K. Ghosh, T. K. Mukherjee, M. G. Mustafa, and R. Ray, Phys. Rev. **D 73**, 114007 (2006).

- [22] C. Ratti, S. Rößner, M. A. Thaler, and W. Weise, *Eur. Phys. J.* **C 49**, 213 (2007) (arXiv: hep-ph/0609218).
- [23] S. Rößner, C. Ratti, and W. Weise, *Phys. Rev.* **D 75**, 034007 (2007) (arXiv: hep-ph/0609281).
- [24] Z. Zhang, and Y. X. Liu, *Phys. Rev.* **C 75**, 064910 (2007) (arXiv: hep-ph/0610221).
- [25] M. Cheng *et al.*, *Phys. Rev.* **D 74**, 054507 (2006).
- [26] T. Kunihiro, *Phys. Lett.* **B 219**, 363 (1989).
- [27] P. Rehberg, S. P. Klevansky, and J. Hüfner, *Phys. Rev.* **C 53**, 410 (1996).
- [28] F. Karsch, *Lect. Notes Phys.* **583**, 209 (2002).
- [29] C. Bernard *et al.* (**MILC** Collaboration), *Phys. Rev.* **D 71**, 034504 (2005).
- [30] M. Buballa, *Phys. Rept.* **407**, 205-376 (2005).
- [31] D. H. Rischke, *Prog. Part. Nucl. Phys.* **52**, 197 (2004).
- [32] K. Fukushima, and Y. Hidaka, *Phys. Rev.* **D 75**, 036002 (2007) (arXiv: hep-ph/0610323).
- [33] C. Sasaki, B. Friman, and K. Redlich, *Phys. Rev.* **D 75**, 074013 (2007) (arXiv: hep-ph/0611147).
- [34] R. D. Pisarski, and F. Wilczek, *Phys. Rev.* **D 29**, 338 (1984).
- [35] H. Hansen, W. M. Alberico, A. Beraudo, A. Molinari, M. Nardi, and C. Ratti, *Phys. Rev.* **D 75**, 065004 (2007).